Mdig suppresses epithelial-mesenchymal transition and inhibits the invasion and metastasis of non-small cell lung cancer via regulating GSK-3β/β-catenin signaling

FENG GENG, ZHANSHI JIANG, XIAOGANG SONG, HAOMIN ZHOU and HONGWEN ZHAO

Department of Pulmonary Medicine, The First Hospital of China Medical University, Shenyang, Liaoning 110001, P.R. China

Received July 16, 2017; Accepted October 2, 2017

DOI: 10.3892/ijo.2017.4154

Abstract. Mineral dust-induced gene (mdig) can inhibit the invasion and metastasis of A549 cells. The main purpose of this study was to explore the molecular mechanism underlying the inhibitory effect of mdig on cell invasion and metastasis. Mdig-knockdown and mdig-overexpressing A549 cells and an mdig-overexpressing human umbilical vein endothelial cell (HUVEC) line were constructed using lentiviral vectors, and western blot analysis was performed to verify the silencing and overexpression of the mdig protein. A Transwell invasion assay was used to detect the invasive abilities of each experimental group, and Transwell migration and scratch assays were used to detect cell migration ability. Western blotting was subsequently conducted to detect the major biochemical indices of the GSK-3β/β-catenin pathway and the protein expression levels and modifications of epithelial-mesenchymal transition (EMT) transcription factors, as well as changes in the expression levels of EMT molecular markers and intercellular adhesion proteins. The results indicated that overexpression of mdig in A549 cells inhibited cell invasion and metastasis, while silencing of mdig increased the invasive and metastatic properties of cells. The molecular mechanism underlying the effects of mdig downregulation on A549 cell invasion and metastasis was found to involve the inhibition of GSK-3β phosphorylation, which in turn promoted the phosphorylation and destabilization of β-catenin. This was associated with downregulation of the downstream transcription factors slug, snail and ZEB1, thus leading to increased expression levels of epithelial cell markers and upregulation of the intercellular adhesion molecules E-cadherin, claudin-1, ZO-1, integrin β1 and integrin β4, which was accompanied by downregulation of the mesenchymal cell markers vimentin and N-cadherin. The HUVECs were used to validate the aforementioned molecular mechanisms and the same conclusions were obtained. The present results indicate that mdig can inhibit the phosphorylation of GSK-3β and promote the phosphorylation and destabilization of β-catenin, in order to suppress the expression of slug, snail, and ZEB1 and the occurrence of EMT, and thereby inhibit the invasion and metastasis of non-small cell lung cancer (NSCLC).

Correspondence to: Professor Hongwen Zhao, Department of Pulmonary Medicine, The First Hospital of China Medical University, No. 155 Nanjing North Street, Heping District, Shenyang, Liaoning 110001, P.R. China
E-mail: hwzhao2007@163.com

Key words: mineral dust-induced gene, non-small cell lung cancer, invasion and metastasis, GSK-3β/β-catenin pathway, epithelial-mesenchymal transition

Introduction

Mineral dust-induced gene (mdig; which is also known as MYC-induced nuclear antigen, mina53 and NO52) is a novel tumor-related gene that has been discovered in the alveolar macrophages of coal miners (1). Many substances can induce mdig expression, such as arsenic (2) and mineral dust (3), among others. It has been reported that mdig is a proto-oncogene that is highly expressed in a variety of tumor cells, where it not only serves as an independent factor leading to tumor formation, but also as a promoter of tumor cell proliferation (1,4-6). Mdig/mina53 is a downstream target gene of the transcription factor c-Myc, and is located on chromosome 3 (3q12.1). The full length mdig gene is composed of 1,510 bases and contains 10 exons that encode 465 amino acids, which amount to a 53-kDa nucleoprotein (1,7). The mdig/mina53 protein contains a conserved JumonjiC (Jmjc) domain that regulates the expression of certain genes in histones through the action of demethylases (8). In a study by Komiya *et al*, NIH-3T3 cells transfected with mdig/mina53 were analyzed using a gene chip technique, which indicated that 125 genes were upregulated and 129 genes were downregulated as a result of mdig overexpression; among the altered genes, 17 were associated with growth factors, 12 were associated with cell proliferation and the cell cycle, 59 were involved in cell invasion and metastasis, 34 were associated with transcriptional regulation, and 20 genes were associated with metabolism (9). It also has been observed that mdig plays an important role in the regulation of cell invasion and metastasis. Our previous study found a contradictory phenomenon: compared with a control group, the expression of mdig in A549 cells increased the ability of the cells to proliferate, while the invasive and metastatic properties of the cells were significantly reduced (6), indicating that mdig can promote the proliferation of tumor cells, but inhibit cell invasion and metastasis; however, the exact mechanism underlying these contradictory findings is not clear.

Epithelial-mesenchymal transition (EMT) is not only a key mechanism in the formation of multi-germ layers and the maintenance of tissue integrity during embryonic development, but is also a key mechanism underlying the invasion and metastasis of tumor cells, the formation of tumor stem cells and tumor resistance (10-14). EMT in tumor cells is primarily characterized by a decrease in intercellular connections, a disappearance of cell polarity and an elongated spindle-like cell morphology, which enables cells to detach and become mobile, and ultimately promotes the occurrence of cell invasion and metastasis (10,15,16). The molecular mechanisms of EMT mainly manifest as a gradual loss of epithelial cell markers (E-cadherin, ZO-1, and claudin-1), a reduction in the expression of cell adhesion proteins (integrin β1, and integrin β4), and an increase in the expression of mesenchymal cell markers (N-cadherin, and vimentin) (10). Previous studies have confirmed that the GSK-3β/β-catenin pathway is an important signal transduction pathway in the regulation of EMT occurrence in cells. Notably, GSK-3β has been reported to phosphorylate β-catenin, while phosphorylation of GSK-3β (P-GSK-3β) inhibits its ability to phosphorylate β-catenin (17,18); non-phosphorylated β-catenin can then translocate into the nucleus and promote the expression of the downstream transcription factors snail, slug and ZEB1, thereby promoting the occurrence of EMT and tumor cell invasion and metastasis (12,19).

The present study demonstrated that mdig can inhibit the phosphorylation of GSK-3β (P-Ser9-GSK-3β) and promote the phosphorylation and destabilization of β-catenin (P-Ser33, Ser37, and Thr41-β-catenin), in order to suppress the expression of slug, snail and ZEB1 and the occurrence of EMT, and thereby inhibit the invasion and metastasis of non-small cell lung cancer (NSCLC).

Materials and methods

Cell culture. The human NSCLC cell line A549 was purchased from the Chinese Academy of Sciences (Shanghai, China). A549 is a tumor cell line originating from alveolar epithelium, with a typical epithelial cell morphology and adherent growth. As a human lung adenocarcinoma cell, A549 cell has been applied widely in EMT study. The human umbilical vein endothelial cells (HUVECs) were purchased from the Peking University Cancer Institute (Beijing, China). HUVEC is an epithelial origin cell line, with a typical epithelial cell morphology, cobblestone appearance with large dark nuclei and adherent growth. This cell line is susceptible to transfection and often used as a tool cell. The cells were cultured in RPMI-1640 culture medium (Hyclone, USA) containing 10% fetal bovine serum (FBS; Hyclone) in a 5% CO_2 cell incubator (Thermo Fisher Scientific, Inc., USA) at 37˚C.

Lentivirus transfection. An mdig overexpression lentiviral vector (LV-mdig; GenBank accession NM_032778), an empty control lentiviral vector (vector), mdig silencing lentiviral vectors (LV-mdig-RNAi 1, sequence: 5'-GGGTGATTTGTT GTACTTT-3'; LV-mdig-RNAi 2, sequence: 5'-AACGATTCA GTTTCACCAA-3') and a control lentiviral vector (LV-con, sequence: 5'-TTCTCCGAACGTGTCACGT-3') were purchased from GeneChem (Shanghai, China). The day before transfection, 5 ml ($5x10^4$ cells/ml) of the target cells were inoculated into a T25 flask (Corning, USA), and when cell confluence reached 30-50%, the cells were incubated with lentivirus concentrations equivalent to the target cell infection index (MOI: A549-50, HUVEC-20). After 16 h, the medium was replenished with 5 ml fresh complete medium and the cells were incubated for a further 48 h. The cells were subsequently analyzed under an inverted fluorescence microscope (Observer A1; ZEISS, Germany), and the transfection efficiency was expressed as the percentage of GFP-positive cells identified with a GFP fluorescence module (excitation, BP470/40; beam splitter, FT495; emission, BP525/50).

Transwell invasion assay. A matrix gel (Matrigel matrix; Corning) was diluted at a 1:3 ratio and spread evenly onto the bottom of 24-well Transwell inserts. A549 cells, and A549 cells transfected with LV-con, LV-mdig and LV-mdig-RNAi were digested and counted during the logarithmic growth phase, and a cell suspension ($1x10^6$ cells/ml) was prepared with serum-free RPMI-1640 cell culture broth. Cell suspension (150 μl) was added to each chamber in a 24-well Transwell plate (Corning), and 600 μl RPMI-1640 medium containing 20% FBS was added to each lower chamber. Subsequently, the upper chambers were inserted into the lower chambers and placed in a 5% CO_2 incubator at 37˚C for 24 h. The upper chambers were then removed and fixed in 4% paraformaldehyde prior to crystal violet staining. Cells were counted in randomly selected visual fields of an inverted fluorescence microscope at x400 magnification.

Transwell migration assay. A549 cells and A549 cells transfected with LV-con, LV-mdig and LV-mdig-RNAi were digested and counted during the logarithmic growth phase, and a cell suspension ($5x10^5$ cells/ml) was prepared with serum-free RPMI-1640 cell culture broth. Cell suspension (150 μl) was added to each chamber in a 24-well Transwell plate (Corning), and 600 μl RPMI-1640 medium containing 20% FBS was added to each lower chamber. Subsequently, the upper chambers were inserted into the lower chambers and placed in a 5% CO_2 incubator at 37˚C for 16 h. The upper chambers were then removed, fixed in 4% paraformaldehyde and stained with crystal violet. Cells were counted in randomly selected visual fields of an inverted fluorescence microscope at x400 magnification.

Wound healing assay. The day before the experiment, A549 cells transfected with LV-con, LV-mdig and LV-mdig-RNAi were digested and counted during the logarithmic growth phase. The cells ($5x10^5$ cells/ml) were incubated in 6-well plates (Corning) for 24 h, and then the cell monolayer was scratched with a 200-μl pipette tip (Coring) positioned at a perpendicular angle to the plate to keep the scratch width consistent. The medium was subsequently removed and the cells were washed three times with PBS (Hyclone), then incubated with serum-free RPMI-1640 medium in a 5% CO_2 incubator at 37˚C. After 0, 12 and 24 h, GFP fluorescence was visualized and the cells were imaged with an inverted fluorescence microscope. ImageJ software (ImageJ 1.51J8, Wayne Rasband, National Institutes of Health, USA) was used to measure the scratch area and calculate the percentage of scratch healing, and the scratch healing areas of the different groups were compared.

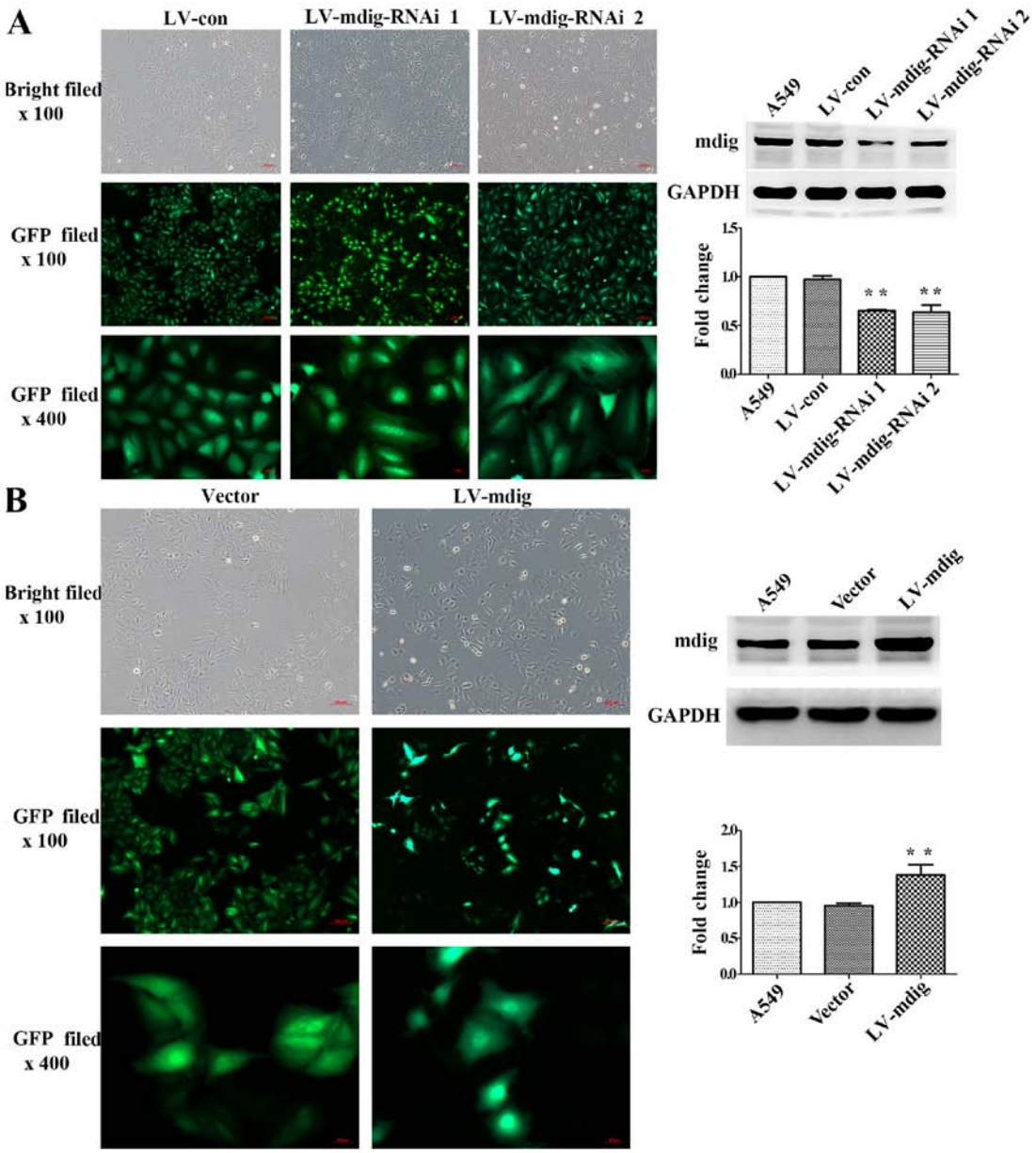

Figure 1. Mdig knockdown and overexpression in A549 cell lines. Transfection efficiency and cell morphology were observed under an inverted fluorescence microscope (for the same field: bright field, x100 magnification; GFP field, x100 and x400 magnification). Western blotting was performed to detect the expression of mdig protein in each group. GAPDH was used as a protein loading control. (A) Stable mdig-silenced A549 cells; the LV-mdig-RNAi 1 and LV-mdig-RNAi 2 groups were compared with the LV-con and A549 groups (**P<0.01). (B) Stable mdig-overexpressing A549 cells; the LV-mdig group was compared with the vector and A549 groups (**P<0.01). Representative images from experiments performed three times.

Western blotting. After 4 passages, total protein was extracted from transfected cells with RIPA buffer containing 10% PMSF, and total protein concentration was measured using a BCA Protein assay kit (Thermo Fisher Scientific, Inc.). The protein samples (30 μg) were subjected to SDS-PAGE (Bio-Rad, USA) and then transferred onto Immobilon-P PVDF membranes (0.45 and 0.22 μm), which were then blocked at room temperature for 2 h with 5% non-fat dried milk. The membranes were subsequently washed with TBST, then incubated with primary antibodies (rabbit mAbs) against mina53 (#173573) (1:1,000; Abcam, USA), phospho-GSK-3β (#5558), integrin β4 (#14803), integrin β1 (#9699), non-phospho (active) β-catenin (non-phospho-Ser33/37/Thr41) (#8814), vimentin (#5741), N-cadherin (#13116), claudin-1 (#13255), β-catenin (#8480), ZO-1 (#8193), snail (#3879), anti-slug (#9585), ZEB1 (#3396), E-cadherin (#3195) and GAPDH (#5174) (1:1,000; Cell Signaling Technology, USA) at 4˚C overnight. After another TBST wash, the membranes were incubated with secondary antibody (#7074) (anti-rabbit IgG; 1:3,000, Cell Signaling Technology) at room temperature for 2 h. Immunoreactive bands were detected with an ECL western blotting system (Clarity Western ECL Substrate; Bio-Rad). The gray scale densities of the bands were measured with ImageJ software, and the density ratio of each protein band to that of GAPDH was calculated and expressed as a percentage relative to the normal control group.

Statistical analysis. The data were expressed as the mean ± standard deviation (SD). Comparisons between groups were performed by a one-way analysis of variance (ANOVA).

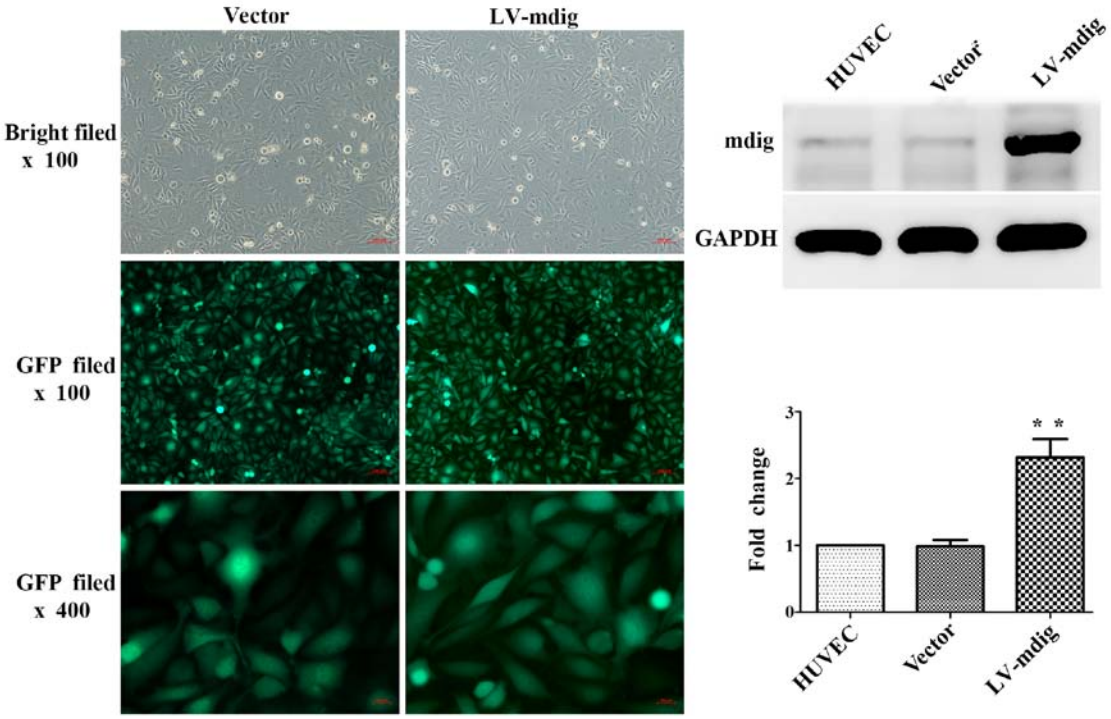

Figure 2. Mdig overexpression in HUVEC line. Transfection efficiency and cell morphology were observed under an inverted fluorescence microscope (for the same field: bright field, x100 magnification; GFP field, x100 and x400 magnification). Western blotting was performed to detect the expression of mdig protein in each group. GAPDH was used as a protein loading control. Stable mdig-overexpressing HUVECs are shown; the LV-mdig group was compared with the vector and HUVEC groups (**P<0.01). Representative images from experiments performed three times.

P<0.05 was considered to indicate a statistically significant difference. Statistical analyses were performed with SPSS 22.0 software for Windows (IBM Corp., Armonk, NY, USA). All experiments were repeated ≥3 times.

Results

Construction of mdig-knockdown and mdig-overexpressing A549 cell lines. Fourth generation A549 cells transfected with lentivirus were observed under the bright field of an inverted fluorescence microscope at x100 magnification. The same fields of view were analyzed for GFP fluorescence at x100 and x400 magnification. All the cell groups exhibited a high cell viability and high transfection efficiency (Fig. 1). In the mdig silencing experiment, cells in the LV-con group exhibited a cobblestone-like cell morphology, while cells in the LV-mdig-RNAi 1 and LV-mdig-RNAi 2 groups exhibited more elongated spindle-like shapes. In addition, mdig protein expression was significantly decreased in the RNAi groups when compared with normal A549 cells and the LV-con group (P<0.01) (Fig. 1A). The LV-mdig-RNAi 1 group was used in the subsequent Transwell assays. In A549 cells overexpressing mdig, the morphology of cells in the LV-mdig group appeared rounder than the cobblestone morphology of cells in the vector group, and mdig protein expression was significantly increased in the LV-mdig group when compared with normal A549 cells and the vector group (P<0.01) (Fig. 1B).

Construction of an mdig-overexpressing HUVEC line. Inverted fluorescence microscopy was used to visualize fourth generation HUVECs transfected with lentivirus as above. All the cell groups exhibited a high cell viability status and high transfection efficiency. There were no marked differences in the morphologies of cells between the LV-mdig and vector groups. However, the expression of mdig protein in the LV-mdig group was significantly upregulated when compared with the normal HUVEC and vector groups (P<0.01) (Fig. 2).

Effect of mdig on the invasion and migration of A549 cells. In this study, Transwell assays were performed to determine the effect of mdig on the invasion and migration of A549 cells. In the invasion assay, there was no significant difference in the number of cells in the matrix layer between the A549 and LV-con groups. By contrast, the number of cells in the LV-mdig group was significantly lower than that in the LV-con and A549 groups (P<0.01), and the number of cells in the LV-mdig-RNAi group was significantly higher than that in the LV-con and A549 groups (P<0.01) (Fig. 3A). The same results were obtained in the migration assay (Fig. 3B).

A scratch-wound assay was performed to further verify the effect of mdig on the migratory ability of A549 cells. In this assay, the LV-mdig group exhibited a significantly slower healing speed than the LV-con group (P<0.05), while the LV-mdig-RNAi group exhibited a significantly faster healing speed than the LV-con group (P<0.05) (Fig. 3C).

Mdig regulates the GSK-3β/β-catenin signaling pathway. In the mdig-knockdown and mdig-overexpressing cell lines, western blotting was performed to analyze the GSK-3β/β-catenin signaling pathway and its downstream regulation of EMT transcriptional regulators. In the mdig knockdown experiment, the expression levels of P-GSK-3β, active β-catenin,

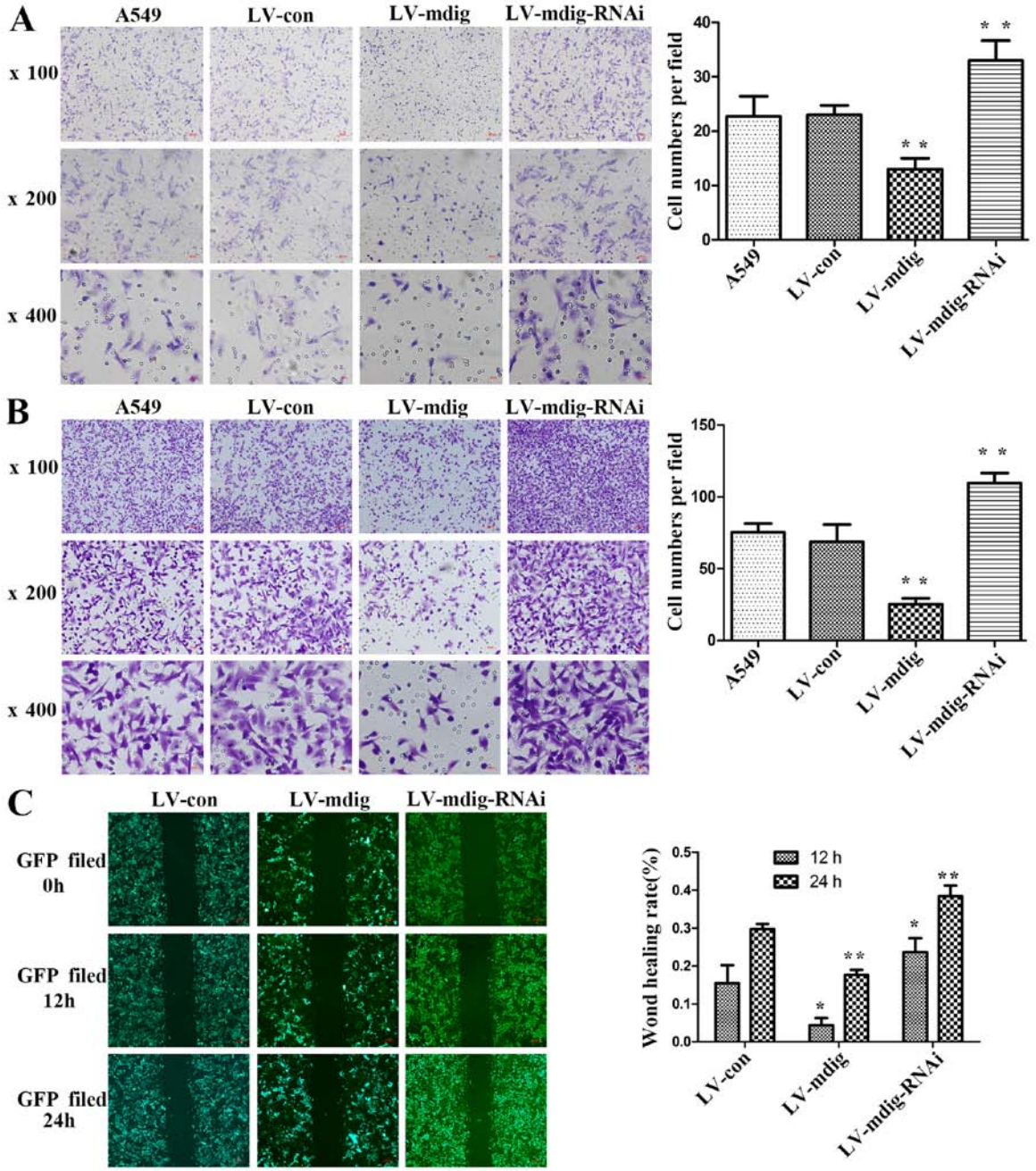

Figure 3. Effect of mdig on the invasion and migration of A549 cells. (A) A Transwell assay was performed to determine the invasive ability of A549 cells; the numbers of transmembrane cells in the LV-mdig and LV-mdig-RNAi groups were compared with those in the LV-con and A549 groups (**P<0.01). (B) A Transwell assay was performed to determine the migratory ability of A549 cells; the numbers of transmembrane cells in the LV-mdig and LV-mdig-RNAi groups were compared with those in the LV-con and A549 groups (**P<0.01). (C) A scatch-wound assay was performed to detect the migratory ability of A549 cells; the percentage of scratch healing in the LV-mdig-RNAi and LV-mdig groups was compared with that in the LV-con group at 12 and 24 h (*P<0.05; **P<0.01). Representative images from experiments performed three times.

slug, snail and ZEB1 in the mdig-knockdown A549 cell group were significantly higher than those in the normal A549 and LV-con groups (P<0.05), while changes in the levels of total β-catenin were not significant (P>0.05) (Fig. 4). In the mdig overexpression experiment, the expression levels of P-GSK-3β, active β-catenin, slug, snail and ZEB1 in mdig-overexpressing A549 cells were significantly lower than those in the normal A549 and LV-con groups (P<0.01), while changes in the levels of total β-catenin were not significant (P>0.05) (Fig. 5). The same results were obtained for mdig-overexpressing HUVECs (Fig. 6). These results show that mdig can inhibit the phosphorylation of GSK-3β and thus promote the phosphorylation of β-catenin. This may reduce the levels of active (non-phosphorylated) β-catenin, leading to a decrease in its direct promotion of the EMT-related factors snail, slug and ZEB1.

Mdig regulates major molecular markers of EMT. Western blotting was used to detect the expression of major EMT markers in the mdig-knockdown and mdig-overexpressing cell lines. In the mdig knockdown experiment, the expression levels of E-cadherin, claudin-1, ZO-1, integrin β1 and integrin β4 in

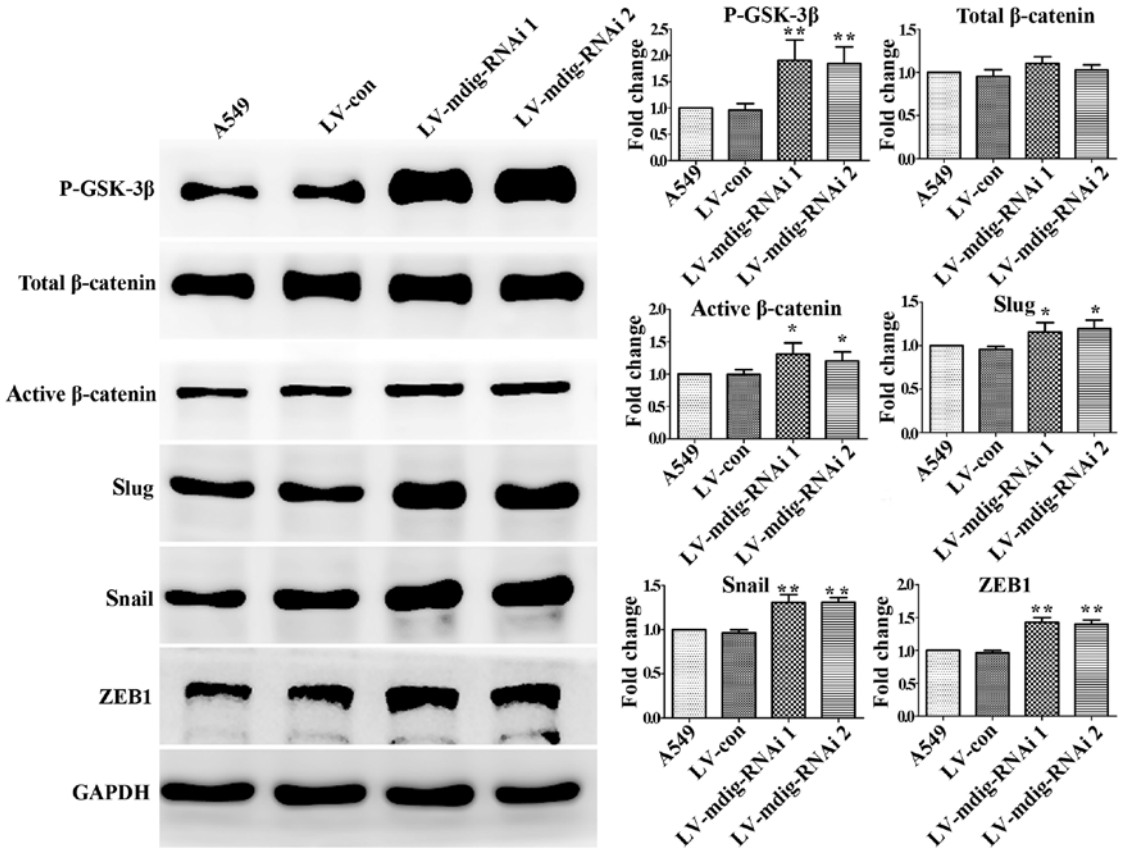

Figure 4. Regulation of the GSK-3β/β-catenin signaling pathway by mdig. Western blotting was used to analyze the GSK-3β/β-catenin signaling pathway and its downstream regulation of EMT-related factors. GAPDH was used as a protein loading control. A549 cell mdig knockdown experiment; the LV-mdig-RNAi 1 and LV-mdig-RNAi 2 groups were compared with the LV-con and A549 groups ($^{*}P<0.05$; $^{**}P<0.01$). Representative images from experiments performed three times.

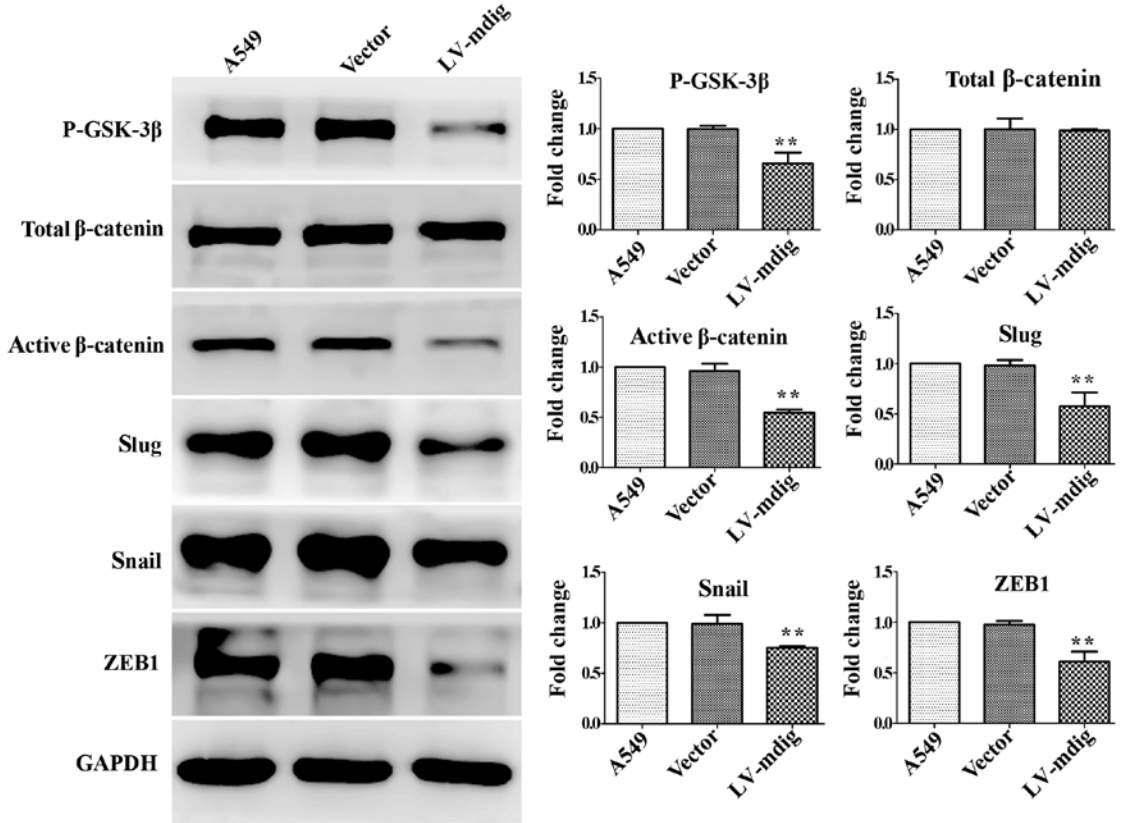

Figure 5. A549 cell mdig overexpression experiment; the LV-mdig group was compared with the vector and A549 groups ($^{**}P<0.01$). Representative images from experiments performed three times.

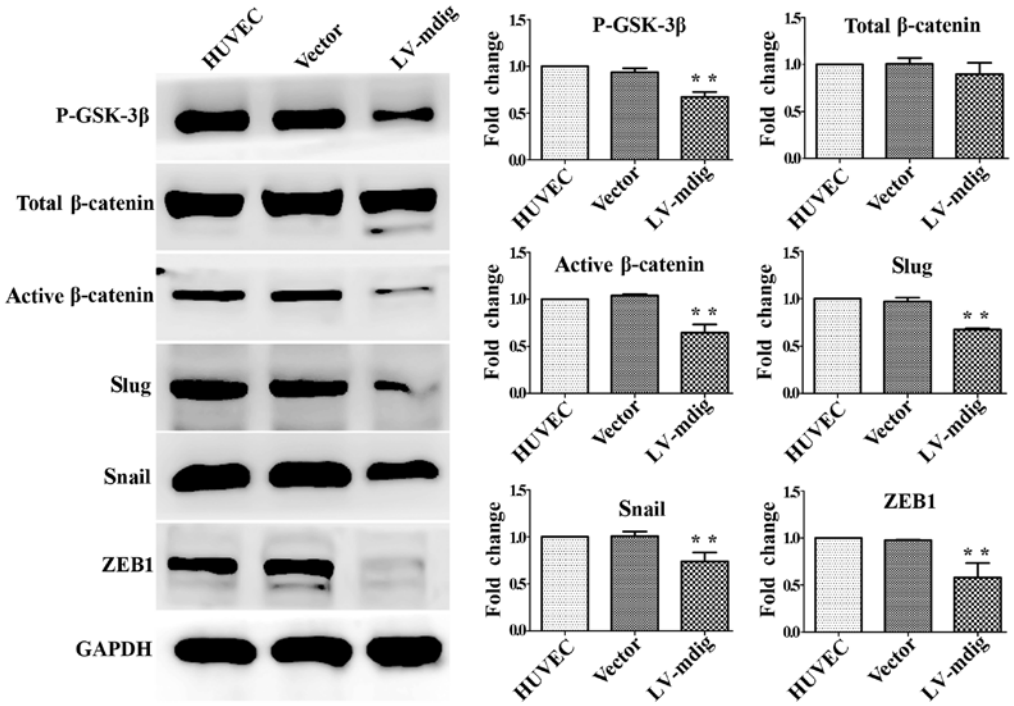

Figure 6. HUVEC mdig overexpression experiment; the LV-mdig group was compared with the vector and HUVEC groups (**P<0.01). Representative images from experiments performed three times.

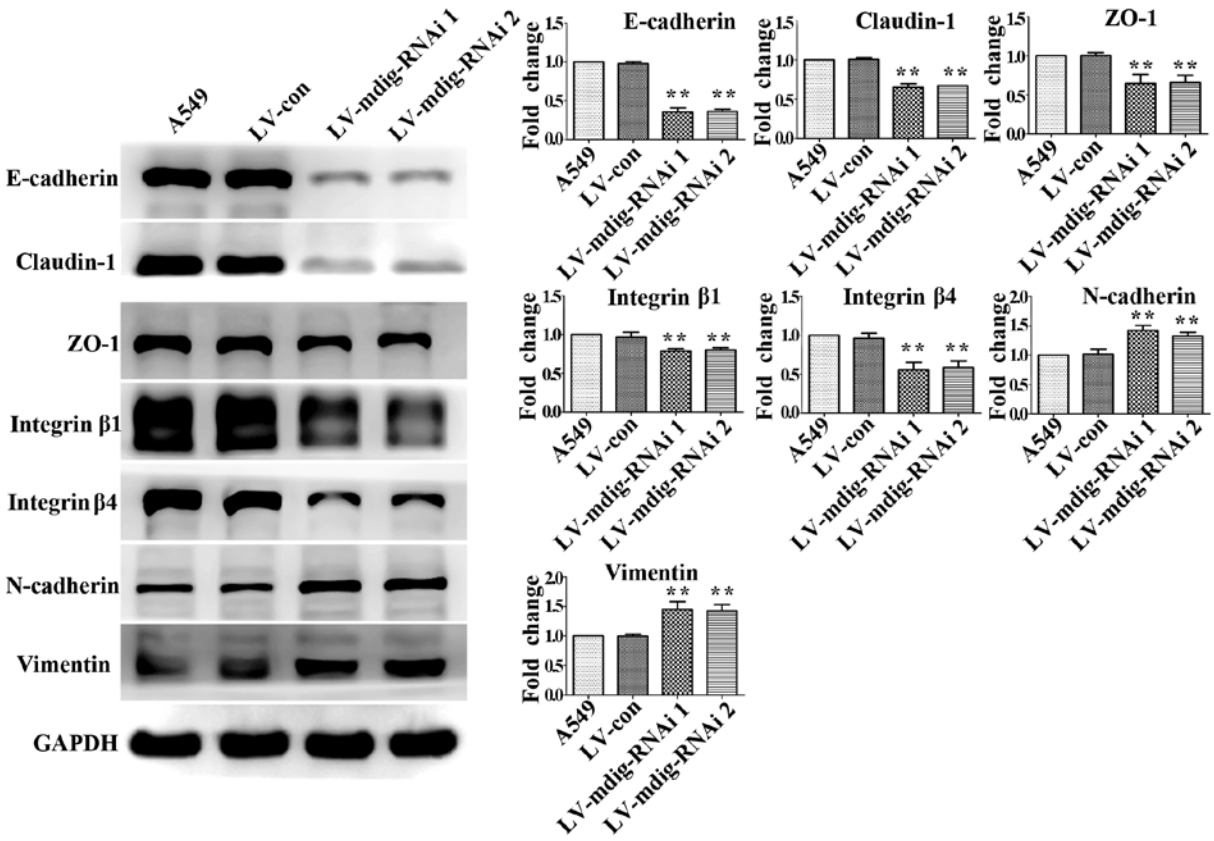

Figure 7. Regulatory effects of mdig on the expression of major EMT markers. Western blotting was used to detect changes in the expression levels of major EMT markers. GAPDH was used as a protein loading control. A549 cell mdig knockdown experiment; the LV-mdig-RNAi 1 and LV-mdig-RNAi 2 groups were compared with the LV-con and A549 groups (**P<0.01). Representative images from experiments performed three times.

mdig-silenced A549 cells were significantly downregulated (P<0.01), while those of N-cadherin and vimentin were significantly upregulated (P<0.01), relative to the A549 and LV-con groups (Fig. 7). Opposite results were obtained for

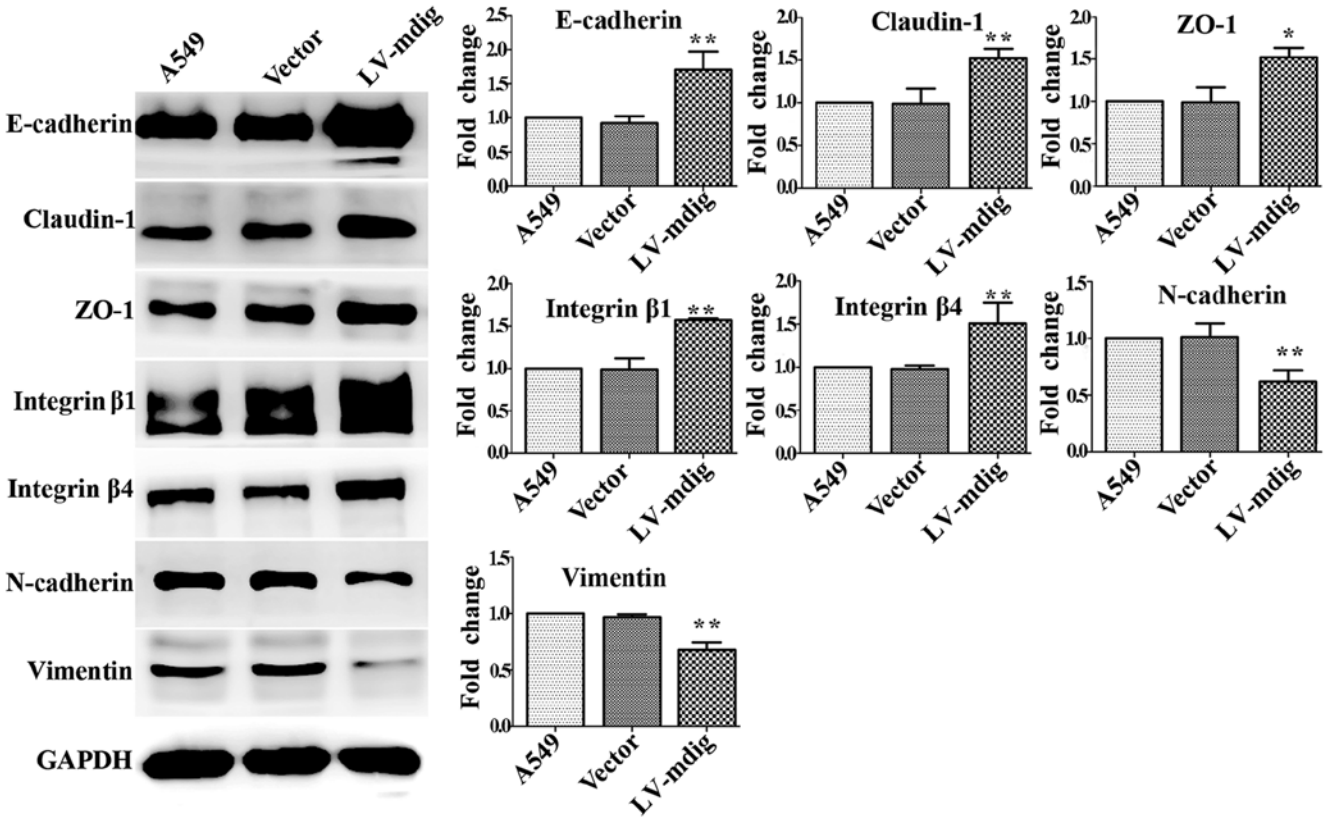

Figure 8. A549 cell mdig overexpression experiment; the LV-mdig group was compared with the vector and A549 groups (*P<0.05; **P<0.01). Representative images from experiments performed three times.

mdig-overexpressing A549 cells; compared with the A549 and LV-con groups, the expression levels of E-cadherin, claudin-1, ZO-1, integrin β1 and integrin β4 were significantly upregulated in mdig-overexpressing A549 cells (P<0.01), while those of N-cadherin and vimentin were significantly downregulated (P<0.01) (Fig. 8). The results for mdig-overexpressing HUVECs were equivalent to those for mdig-overexpressing A549 cells (Fig. 9); mdig overexpression was able to upregulate the epithelial cell markers E-cadherin, claudin-1, ZO-1, integrin β1 and integrin β4 (P<0.05), while downregulating the expression of the mesenchymal cell markers N-cadherin and vimentin (P<0.01).

Discussion

Lung cancer has become one of the world's highest ranked malignancies in terms of morbidity and mortality rates, and thus is a serious threat to human health and quality of life. Smoking, environmental pollution and occupational, physical and chemical carcinogen exposure have all been identified as risk factors of lung cancer (20,21). It is presently established that the occurrence and development of human lung cancer is due to a large number of genetic changes. Mdig is a lung cancer-related gene that is highly expressed in lung cancer tissues and most lung cancer cell lines, but not in normal lung tissues, and can be induced by environmental stimuli in alveolar macrophages (1). Previous studies have confirmed that mdig is a proto-oncogene that exhibits high expression in a variety of tumors, and serves key roles in promoting tumor cell proliferation. The main reason for the high mortality rate of cancer patients is due to the invasion and metastasis of tumor cells; however, current research on mdig regarding its potential regulation of cell invasion and metastasis is limited. Our previous study found that the overexpression of mdig in A549 cells significantly increased cell proliferation, but significantly reduced cell invasion and migration (6). These data indicated that mdig can promote tumor cell proliferation while inhibiting cell invasion and metastasis; however, the exact mechanism underlying these contradicting effects is not clear. The study also found that the expression levels of mdig and the overall survival (OS) rate of lung cancer patients were inversely related, with high expression levels of mdig indicating a poor prognosis alongside the stimulatory effects on cell proliferation. However, when patients were classified according to the American Joint Committee on Cancer (AJCC) staging system for lymph node metastasis status (N), we noted that higher mdig expression only predicted a poorer OS rate of patients with AJCC N0 (no regional lymph node metastasis) and AJCC N1 (possible proximal lymph node metastasis), but not for those with AJCC N2 (distant lymph node metastasis). Therefore, although these findings were statistically insignificant, higher mdig expression appears to predict a better, rather than poorer, survival rate for AJCCN2 patients, which may support the findings that mdig is an inhibitory factor for cell migration and invasion (6). Komiya *et al* also confirmed that mdig/mina53 may be a prognostic indicator of lung cancer; they found that the expression of mdig was markedly increased in early squamous cell carcinoma,

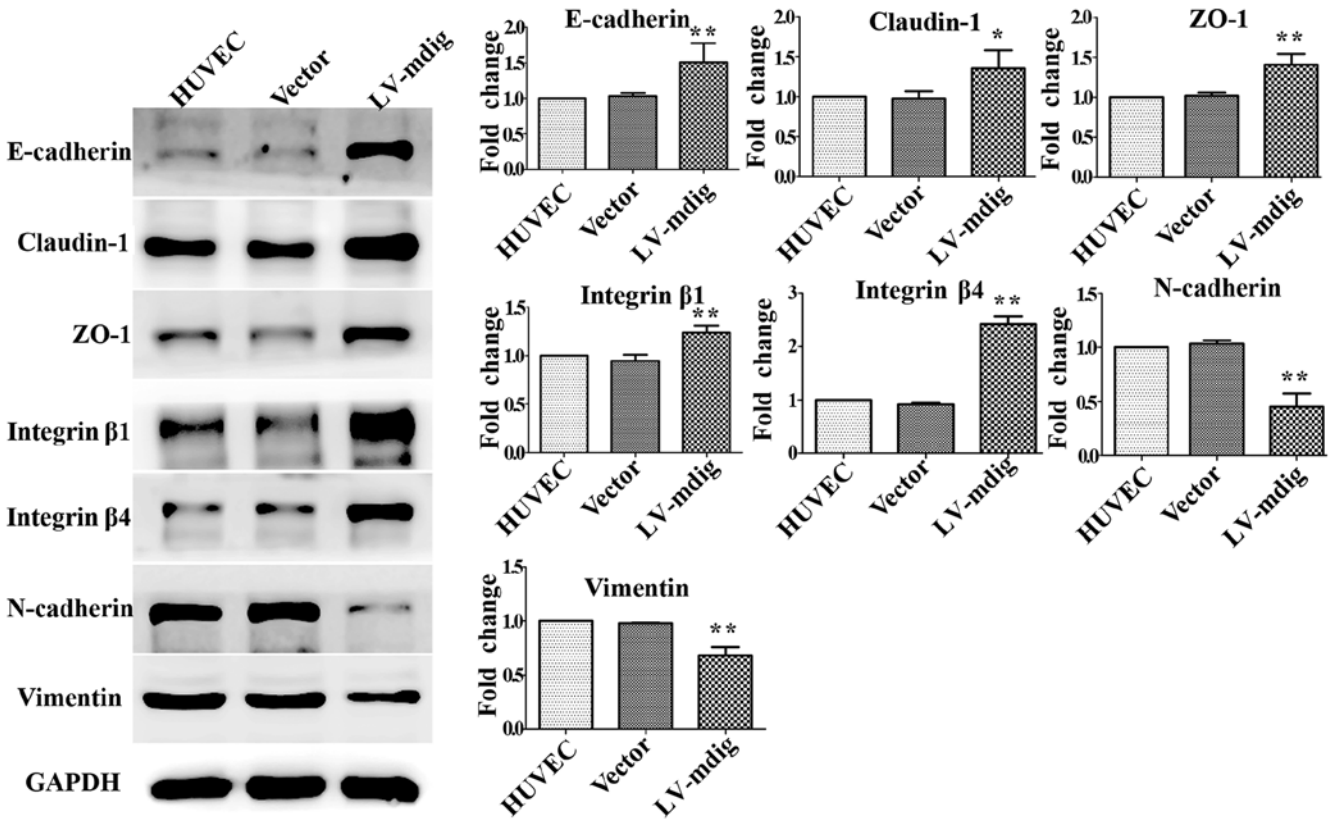

Figure 9. HUVEC mdig overexpression experiment; the LV-mdig group was compared with the vector and HUVEC groups (*P<0.05; **P<0.01). Representative images from experiments performed three times.

and that NSCLC patients positive for mdig/mina53 expression had a better prognosis than mdig-negative patients, which indicated that mdig/mina53 may inhibit tumor cell invasion and metastasis and promote apoptosis (9). These findings are in accordance with our previous study, and suggest that mdig has the ability to inhibit tumor cell invasion and metastasis in NSCLC; however, the corresponding molecular mechanism is not clear.

Tumor cell invasion and metastasis may occur to varying degrees during the different stages of EMT. Notably, the occurrence of EMT has been associated with NSCLC invasion and translocation (10). Studies have shown that morphological changes are induced by EMT in tumor cells; when EMT occurs in A549 cells, the morphology of cells changes from a cobblestone shape to an elongated spindle-like shape characteristic of fibroblastoid cells (16). In order to investigate the mechanism underlying the regulatory effects of mdig on the invasion and metastasis of A549 cells, the present study constructed mdig-silenced and mdig-overexpressing A549 cell lines. It was observed that the morphology of mdig-silenced A549 cells changed from a cobblestone shape to an elongated spindle-like shape (i.e., a fibroblastoid appearance), while the morphology of mdig-overexpressing A549 cells became rounder in appearance compared with the initial cobblestone shape, thus indicating that the expression of mdig plays an important role in the morphological changes of A549 cells. On the basis of the aforementioned findings, Transwell assays were performed to determine the effects of mdig silencing and overexpression on the invasion and migration of A549 cells. The results of the invasion experiment demonstrated that mdig overexpression significantly decreased the number of cells that invaded through the matrix and membrane, while mdig knockdown significantly increased the number of cells when compared with the normal A549 and control groups. Identical results were obtained from the migration experiment. In order to further verify the effect of mdig on the migratory ability of A549 cells, a scratch-wound assay was performed. Compared with the control group, the mdig overexpression A549 cell group exhibited a significantly slower healing rate, and the mdig knockdown group exhibited a significantly faster healing rate. Therefore, mdig overexpression can inhibit the invasion and metastasis of A549 cells, and silencing of mdig can increase the invasive and migratory properties of cells, suggesting that mdig has the ability to inhibit the invasion and metastasis of A549 cells.

In order to further explore the mechanism underlying these inhibitory effects of mdig, this study examined the effect of mdig on the expression of the GSK-3β/β-catenin signaling axis, the downstream transcription factors snail, slug and ZEB1, and the major molecular markers of EMT. The results showed that mdig could inhibit the phosphorylation of GSK-3β at Ser9 and promote the phosphorylation of β-catenin, which resulted in a decrease in the active (non-phospho at Ser33, Ser37 and Thr41) form of β-catenin, leading to a reduction in the direct promotion of slug, snail and ZEB1. Our results indicated that the regulation of mdig on the signaling pathway was mainly post-translational modification. Mdig could also upregulate

epithelial cell markers (E-cadherin, claudin-1 and ZO-1) and mediate the expression of integrin β1 and integrin β4, the key facilitators of extracellular matrix adhesion, while downregulating mesenchymal cell markers (N-cadherin and vimentin). These results suggested that mdig can promote the phosphorylation of β-catenin by inhibiting the phosphorylation of GSK-3β, in order to suppress the expression of slug, snail and ZEB1 and the occurrence of EMT, and thereby inhibit the invasion and metastasis of NSCLC. The present study also used HUVEC cells to verify the above molecular mechanisms, and the same conclusions were obtained. Collectively, our results elucidated the molecular mechanism underlying the inhibitory effects of mdig on the invasion and metastasis of NSCLC by demonstrating a strong correlation between the expression levels of mdig and the examined proteins in tumor cells and normal cells, as observed previously (6,9), and supported the clinical findings that mdig-positive NSCLC is associated with a better prognosis than the mdig-negative form in patients at the advanced stage because of mdig inhibiting invasion and metastasis of NSCLC (22). The present study focused on the regulation of tumor cell biological behavior by mdig, and advanced our understanding of the underlying regulatory mechanism regarding downstream target genes. However, the correlation between the expression levels of mdig and the examined proteins in patient samples and whether it is only through GSK-3β/β-catenin pathway for mdig to affect the invasion and migration of NSCLC need to be studied in the future. It should be noted that positive mdig expression in other types of tumors, such as breast cancer (23), liver cancer (24), gastric cancer (25,26), neuroblastoma (27), renal cell carcinoma (28), and esophageal squamous cell carcinoma (29,30), is a poor prognostic indicator. Mdig expression is not significantly associated with the prognosis of some tumors, such as primary gingival squamous cell carcinoma (31). However, in general, mdig is considered to be an important factor associated with important tumor-related genes, and not only exhibits different functions during different tumor stages, but also in different tumor tissues (32). Future research should further explore the molecular mechanisms of mdig in tumor cell behavior, and also focus on the value of mdig in the diagnosis, staging, treatment and prognosis of tumors.

Acknowledgements

This study was supported by the National Natural Science Foundation of China (grant no. 81472194) and by the Project of Liaoning Distinguished Professor [grant no. (2013) 204] to Hongwen Zhao.

References

1. Zhang Y, Lu Y, Yuan BZ, Castranova V, Shi X, Stauffer JL, Demers LM and Chen F: The Human mineral dust-induced gene, mdig, is a cell growth regulating gene associated with lung cancer. Oncogene 24: 4873-4882, 2005.
2. Sun J, Yu M, Lu Y, Thakur C, Chen B, Qiu P, Zhao H and Chen F: Carcinogenic metalloid arsenic induces expression of mdig oncogene through JNK and STAT3 activation. Cancer Lett 346: 257-263, 2014.
3. Wu K, Li L, Thakur C, Lu Y, Zhang X, Yi Z and Chen F: Proteomic characterization of the World Trade Center dust-activated mdig and c-myc signaling circuit linked to multiple myeloma. Sci Rep 6: 36305, 2016.
4. Ma D, Guo D, Li W and Zhao H: Mdig, a lung cancer-associated gene, regulates cell cycle progression through p27(KIP1). Tumour Biol 36: 6909-6917, 2015.
5. Tan XP, Dong WG, Zhang Q, Yang ZR, Lei XF and Ai MH: Potential effects of Mina53 on tumor growth in human pancreatic cancer. Cell Biochem Biophys 69: 619-625, 2014.
6. Yu M, Sun J, Thakur C, Chen B, Lu Y, Zhao H and Chen F: Paradoxical roles of mineral dust induced gene on cell proliferation and migration/invasion. PLoS One 9: e87998, 2014.
7. Tsuneoka M, Koda Y, Soejima M, Teye K and Kimura H: A novel myc target gene, mina53, that is involved in cell proliferation. J Biol Chem 277: 35450-35459, 2002.
8. Chen B, Yu M, Chang Q, Lu Y, Thakur C, Ma D, Yi Z and Chen F: Mdig de-represses H19 large intergenic non-coding RNA (lincRNA) by down-regulating H3K9me3 and heterochromatin. Oncotarget 4: 1427-1437, 2013.
9. Komiya K, Sueoka-Aragane N, Sato A, Hisatomi T, Sakuragi T, Mitsuoka M, Sato T, Hayashi S, Izumi H, Tsuneoka M, *et al*: Mina53, a novel c-Myc target gene, is frequently expressed in lung cancers and exerts oncogenic property in NIH/3T3 cells. J Cancer Res Clin Oncol 136: 465-473, 2010.
10. Heerboth S, Housman G, Leary M, Longacre M, Byler S, Lapinska K, Willbanks A and Sarkar S: EMT and tumor metastasis. Clin Transl Med 4: 6, 2015.
11. Yilmaz M and Christofori G: EMT, the cytoskeleton, and cancer cell invasion. Cancer Metastasis Rev 28: 15-33, 2009.
12. Brabletz T, Hlubek F, Spaderna S, Schmalhofer O, Hiendlmeyer E, Jung A and Kirchner T: Invasion and metastasis in colorectal cancer: Epithelial-mesenchymal transition, mesenchymal-epithelial transition, stem cells and beta-catenin. Cells Tissues Organs 179: 56-65, 2005.
13. Thiery JP, Acloque H, Huang RY and Nieto MA: Epithelial-mesenchymal transitions in development and disease. Cell 139: 871-890, 2009.
14. Cuyàs E, Corominas-Faja B and Menendez JA: The nutritional phenome of EMT-induced cancer stem-like cells. Oncotarget 5: 3970-3982, 2014.
15. Godde NJ, Galea RC, Elsum IA and Humbert PO: Cell polarity in motion: Redefining mammary tissue organization through EMT and cell polarity transitions. J Mammary Gland Biol Neoplasia 15: 149-168, 2010.
16. Ren ZX, Yu HB, Li JS, Shen JL and Du WS: Suitable parameter choice on quantitative morphology of A549 cell in epithelial-mesenchymal transition. Biosci Rep 35: 35, 2015.
17. Yost C, Torres M, Miller JR, Huang E, Kimelman D and Moon RT: The axis-inducing activity, stability, and subcellular distribution of beta-catenin is regulated in *Xenopus* embryos by glycogen synthase kinase 3. Genes Dev 10: 1443-1454, 1996.
18. Morin PJ, Sparks AB, Korinek V, Barker N, Clevers H, Vogelstein B and Kinzler KW: Activation of beta-catenin-Tcf signaling in colon cancer by mutations in beta-catenin or APC. Science 275: 1787-1790, 1997.
19. Peinado H, Olmeda D and Cano A: Snail, Zeb and bHLH factors in tumour progression: An alliance against the epithelial phenotype? Nat Rev Cancer 7: 415-428, 2007.
20. Chen W, Zheng R, Baade PD, Zhang S, Zeng H, Bray F, Jemal A, Yu XQ and He J: Cancer statistics in China, 2015. CA Cancer J Clin 66: 115-132, 2016.
21. Siegel RL, Miller KD and Jemal A: Cancer statistics, 2016. CA Cancer J Clin 66: 7-30, 2016.
22. Komiya K, Sueoka-Aragane N, Sato A, Hisatomi T, Sakuragi T, Mitsuoka M, Sato T, Hayashi S, Izumi H, Tsuneoka M, *et al*: Expression of Mina53, a novel c-Myc target gene, is a favorable prognostic marker in early stage lung cancer. Lung Cancer 69: 232-238, 2010.
23. Thakur C, Lu Y, Sun J, Yu M, Chen B and Chen F: Increased expression of mdig predicts poorer survival of the breast cancer patients. Gene 535: 218-224, 2014.
24. Huo Q, Ge C, Tian H, Sun J, Cui M, Li H, Zhao F, Chen T, Xie H, Cui Y, *et al*: Dysfunction of IKZF1/MYC/MDIG axis contributes to liver cancer progression through regulating H3K9me3/p21 activity. Cell Death Dis 8: e2766, 2017.
25. Xing J, Wang K, Liu PW, Miao Q and Chen XY: Mina53, a novel molecular marker for the diagnosis and prognosis of gastric adenocarcinoma. Oncol Rep 31: 634-640, 2014.
26. Ogasawara S, Komuta M, Nakashima O, Akiba J, Tsuneoka M and Yano H: Accelerated expression of a Myc target gene Mina53 in aggressive hepatocellular carcinoma. Hepatology Res 40: 330-336, 2010.

27. Fukahori S, Yano H, Tsuneoka M, Tanaka Y, Yagi M, Kuwano M, Tajiri T, Taguchi T, Tsuneyoshi M and Kojiro M: Immunohistochemical expressions of Cap43 and Mina53 proteins in neuroblastoma. J Pediatr Surg 42: 1831-1840, 2007.
28. Ishizaki H, Yano H, Tsuneoka M, Ogasawara S, Akiba J, Nishida N, Kojiro S, Fukahori S, Moriya F, Matsuoka K, *et al*: Overexpression of the myc target gene Mina53 in advanced renal cell carcinoma. Pathol Int 57: 672-680, 2007.
29. Teye K, Arima N, Nakamura Y, Sakamoto K, Sueoka E, Kimura H and Tsuneoka M: Expression of Myc target gene mina53 in subtypes of human lymphoma. Oncol Rep 18: 841-848, 2007.
30. Tsuneoka M, Fujita H, Arima N, Teye K, Okamura T, Inutsuka H, Koda K, Shirouzu K and Kimura H: Mina53 as a potential prognostic factor for esophageal squamous cell carcinoma. Clin Cancer Res 10: 7347-7356, 2004.
31. Kuratomi K, Yano H, Tsuneoka M, Sakamoto K, Kusukawa J and Kojiro M: Immunohistochemical expression of Mina53 and Ki67 proteins in human primary gingival squamous cell carcinoma. Kurume Med J 53: 71-78, 2006.
32. Thakur C and Chen F: Current understanding of mdig/MINA in human cancers. Genes Cancer 6: 288-302, 2015.